

## Electronic and optical properties of ordered $\text{Be}_x\text{Zn}_{1-x}\text{Se}$ alloys by the FPLAPW method

This article has been downloaded from IOPscience. Please scroll down to see the full text article.

2008 J. Phys.: Condens. Matter 20 075205

(<http://iopscience.iop.org/0953-8984/20/7/075205>)

View [the table of contents for this issue](#), or go to the [journal homepage](#) for more

Download details:

IP Address: 129.252.86.83

The article was downloaded on 29/05/2010 at 10:34

Please note that [terms and conditions apply](#).

# Electronic and optical properties of ordered $\text{Be}_x\text{Zn}_{1-x}\text{Se}$ alloys by the FPLAPW method

S Kumar<sup>1</sup>, Tarun K Maurya<sup>1</sup> and S Auluck<sup>2</sup>

<sup>1</sup> Physics Department, Institute of Engineering and Technology, M J P Rohilkhand University, Bareilly-243 006, India

<sup>2</sup> Physics Department, Indian Institute of Technology, Kanpur-208016, U.P, India

E-mail: [drsudhirkumar.in@gmail.com](mailto:drsudhirkumar.in@gmail.com)

Received 14 October 2007, in final form 15 December 2007

Published 25 January 2008

Online at [stacks.iop.org/JPhysCM/20/075205](http://stacks.iop.org/JPhysCM/20/075205)

## Abstract

We have used the *ab initio* full potential linear augmented plane wave (FPLAPW) method within the local density functional theory to calculate the dielectric function and reflectivity of  $\text{Be}_x\text{Zn}_{1-x}\text{Se}$  alloys for different compositions  $x = 0.0, 0.25, 0.50, 0.75$  and  $1.0$ . The calculated dielectric function and reflectivities show reasonably good agreement with the experimental data. The valence band maximum is dominated by the Se-3p states and the conduction band minimum by Zn-4s states for  $x = 0.0$ , i.e. ZnSe, and by Be-p states for  $x = 1.0$ , i.e. BeSe. Our calculations show that the direct band gap varies linearly with  $x$ .

## 1. Introduction

There is an increasing demand for good semiconductors for various electrical and optical devices. Keeping this in mind the group IV and III–V compounds have been extensively studied theoretically as well as experimentally. Recently, there has been a dedicated effort to understand the II–VI compounds. In fact, Be compounds and their alloys remain unexplored because of their highly toxic nature. Alloying of BeSe with ZnSe offers an opportunity to create a new family of wide band gap semiconductors with band gaps varying from 2.7 to 5.2 eV. The performance and lifetime of devices depend on the doping material.

Doping of Be in ZnSe (i.e.  $\text{Be}_x\text{Zn}_{1-x}\text{Se}$  ternary alloys) has been suggested by Waag *et al* [1]. It improves the hardness [2, 3] of the materials which is related to a longer lifetime for devices. At the same time, smaller beryllium concentrations are required to obtain large band gaps and have a lattice matched with GaAs [4]. The large band gap of BeSe (5.15 eV) suggests the possibility of using these materials for ultraviolet (UV) optoelectronic applications. Molecular beam epitaxy (MBE) [5] has made possible the preparation of semiconductor-grade films of  $\text{Be}_x\text{Zn}_{1-x}\text{Se}$  alloys. Bosang *et al* [6] have grown  $\text{Be}_x\text{Zn}_{1-x}\text{Se}$  alloys by the MBE technique and studied photoluminescence (PL) as a function of temperature and pressure. Mintairov *et al* [7] have grown  $\text{Be}_x\text{Zn}_{1-x}\text{Se}$  alloys by MBE on GaAs (001) substrate of thickness between

0.3–1 mm and have studied IR and Raman spectra. Chauvet *et al* [8] have grown  $\text{Be}_x\text{Zn}_{1-x}\text{Se}$  on GaAs(100) substrate by MBE and studied low temperature photoluminescence and reflectivity to locate the direct to indirect band gap cross-over. Wilmers *et al* [9] have grown  $\text{Be}_x\text{Zn}_{1-x}\text{Se}$  on GaAs substrate by using MBE and have measured the dielectric function for the full composition range (i.e.  $x = 0.0$ – $1.0$ ) by ellipsometric spectroscopy at room temperature.

Theoretical calculation of the optical and electronic properties of  $\text{BeX}$  ( $X = \text{Te}, \text{Se}$  and  $\text{S}$ ) compounds were performed by Stukel [10]. The calculated dielectric functions were not compared with the experimental data because no data were available at that time. A few non-relativistic local density approximation (LDA) calculations of the structural, electronic and optical properties have been performed [11, 12] for beryllium monochalcogenides. Baaziz *et al* [13] have calculated the composition dependent structural and electronic properties of  $\text{Be}_x\text{Zn}_{1-x}\text{Se}$  alloys. Fleszar and Hanke [14] have calculated electronic excitations in  $\text{BeX}$  using the many-body Green's functions technique (GW) and have given a detailed discussion of LDA versus GW. The vibrational properties of  $\text{Be}_x\text{Zn}_{1-x}\text{Se}$  alloys have been studied by Postnikov *et al* [15] using the SIESTA code [16] with norm-conserving pseudopotentials and localized basis functions. Recently, Berghout *et al* [17] studied  $\text{Zn}_{1-x}\text{Be}_x\text{Se}$  using a plane-wave pseudopotential scheme [18]. Their work shows that the lattice constants follow Vegard's law.

**Table 1.** Lattice constants (in Å) for  $\text{Be}_x\text{Zn}_{1-x}\text{Se}$  alloys.

System	Present calculation <sup>a</sup>	WIEN2K <sup>b</sup>	WIEN2K <sup>c</sup>	Previous study	Expt.
ZnSe	5.667	5.7598	5.6998	5.633 <sup>d</sup> , 5.638 <sup>e</sup> , 5.743 <sup>f</sup> , 5.635 <sup>h</sup> , 5.645 <sup>i</sup> , 5.543 <sup>j</sup> , 5.568 <sup>k</sup> , 5.571 <sup>l</sup> , 5.5876 <sup>m</sup> , 5.59 <sup>n</sup>	5.667 <sup>g</sup>
$\text{Be}_{0.25}\text{Zn}_{0.75}\text{Se}$	5.5363	5.6371	5.5872	5.632 <sup>f</sup>	
$\text{Be}_{0.50}\text{Zn}_{0.50}\text{Se}$	5.4055	5.4805	5.4671	5.505 <sup>f</sup>	
$\text{Be}_{0.75}\text{Zn}_{0.25}\text{Se}$	5.2747	5.3346	5.3239	5.359 <sup>f</sup>	
BeSe	5.144	5.2282	5.1913	5.144 <sup>o</sup> , 5.037 <sup>p</sup> , 5.183 <sup>q</sup> , 5.037 <sup>r</sup>	5.144 <sup>q</sup>

<sup>a</sup> Lattice constants calculated using Vegard's law; <sup>b</sup> Unrelaxed atomic positions;

<sup>c</sup> Relaxed atomic positions; <sup>d</sup> Reference [28], LMTO;

<sup>e</sup> Reference [29], pseudopotential within LDA; <sup>f</sup> Reference [13], WIEN2K;

<sup>g</sup> Reference [30]; <sup>h</sup> Reference [31]; <sup>i</sup> Reference [32], pseudopotential plane wave method;

<sup>j</sup> Reference [32], pseudopotential plane wave method with NLCC<sub>s</sub>;

<sup>k</sup> Reference [15], WIEN2K(LDA); <sup>l</sup> Reference [15], WIEN2K(GGA);

<sup>m</sup> Reference [15], SIESTA; <sup>n</sup> Reference [17], pseudopotential scheme;

<sup>o</sup> Reference [12], WIEN97;

<sup>p</sup> Reference [11], pseudopotential within LDA; <sup>q</sup> Reference [14]; <sup>r</sup> Reference [33].

To the best of our knowledge no detailed calculations of the optical properties have been performed for the  $\text{Be}_x\text{Zn}_{1-x}\text{Se}$  alloys. Hence we thought it worthwhile to perform such calculations, especially since experimental data are available.

In this paper we report such calculations using the state of the art full potential linear augmented plane wave method (FPLAPW). This paper is organized as follows. In section 2, we give details of our calculations. The projected density of states and frequency dependent dielectric properties (relaxed and unrelaxed) are presented and discussed in section 3. Section 4 summarizes our conclusions.

## 2. Method of calculation

We have calculated the optical properties of cubic  $\text{Be}_x\text{Zn}_{1-x}\text{Se}$  alloys using the FPLAPW method [19] in a scalar relativistic version as implemented in the WIEN2K package [20]. For the exchange correlations, we have used the generalized gradient approximation (GGA) [21]. In the FPLAPW method, a basis set is obtained by dividing the unit cell into non-overlapping atomic spheres (centered on the atomic sites) and an interstitial region. Inside the atomic sphere, a linear combination of radial function times spherical harmonic is used, and in the interstitial region a plane wave expansion is augmented by an atomic like function in every atomic sphere. This method yields accurate energy eigenvalues and wavefunctions, therefore appropriate for calculating the electronic and optical properties of crystalline solids. We have chosen sphere radii of 1.8, 2.0, and 2.1 au for Be, Zn and Se, respectively. The values of  $K_{\max} \times R_{\text{MT}} = 7.0$  (where  $R_{\text{MT}}$  is the atomic sphere radius and  $K_{\max}$  is the interstitial plane wave cut-off),  $G_{\max} = 14$  (used in charge density Fourier expansion) and  $l_{\max} = 10$  (for wavefunction expansions inside the sphere) are kept constant throughout the calculations.

A cubic unit cell is constructed with four group II atoms (Zn/Be) and four group VI atoms (Se). We have considered  $\text{Be}_x\text{Zn}_{1-x}\text{Se}$  alloys as having cubic symmetry in

our calculation for all the five systems to maintain consistency and simplicity. We expect that for  $x = 0.5$  the alloy is a layered structure and should be non-cubic. We have taken four layers and hence a cubic unit cell. For  $x = 0.25, 0.50, 0.75$  we have replaced one, two and three Zn atoms, respectively, by Be to get the desired concentration. The idea of constructing an alloy by taking a large unit cell (cubic eight-atom) and repeating it three dimensionally for the calculation of the electronic structure of the semiconductor alloy has been used by Agrawal *et al* [22]. Recently, Ahuja *et al* [23] have used an eight-atom cubic supercell to calculate the optical properties of  $\text{Be}_x\text{Zn}_{1-x}\text{Te}$  alloys, although no such calculations have been performed for  $\text{Be}_x\text{Zn}_{1-x}\text{Se}$  alloys.

It is expected that spin-orbit coupling (SOC) plays an important role in the optical properties of  $\text{Be}_x\text{Zn}_{1-x}\text{Se}$  alloys. We have calculated the optical properties of ZnSe including SOC. It has been observed that there is a negligible or minor effect on the optical properties. On the scale that we show our results, there is hardly any discernible difference. We have chosen ZnSe to test the SOC effect because in other alloys Zn is replaced by Be where SOC is smaller. Self-consistency was obtained using 216  $k$ -points in the irreducible Brillouin zone (IBZ). The Brillouin zone integrations were carried out using the tetrahedron method [24].

For the calculation of the optical properties, the crystal structures are optimized by force and stress minimization in which the atoms are allowed to move towards the equilibrium positions. The Hellman-Feynman forces acting on each atom are calculated and the structure is relaxed in all directions until these forces become smaller than 0.1 mRyd/au. The total energies converged to below  $10^{-4}$  eV with respect to the Brillouin zone integration. Thereafter the lattice constants are optimized. These are presented in table 1. We have also calculated total energies using 27, 64 and 125  $k$ -points in the IBZ and do not find any significant differences, suggesting that our results are well converged with respect to the number of  $k$ -points. A dense mesh of 512  $k$ -points in the IBZ has been

used for the calculation of optical properties. In a cubic unit cell only one component of the dielectric function has to be calculated, i.e.  $\epsilon_{xx}$ , written as

$$\epsilon(\omega) = \epsilon_1(\omega) + i\epsilon_2(\omega) \quad (1)$$

describes the optical response of the system at all photon energies  $E = \hbar\omega$ . The imaginary part of the dielectric function  $\epsilon_2(\omega)$  is given by [25]

$$\epsilon_2(\omega) = \left(\frac{4\pi e^2}{m^2\omega^2}\right) \sum_{ij} \int |i|M|j|^2 f_i(1-f_j) \times \delta(E_F - E_i - \omega) d^3k, \quad (2)$$

where  $M$  is the dipole matrix element,  $i$  and  $j$  are the initial and final states, respectively,  $f_i$  is the Fermi distribution function for the  $i^{\text{th}}$  state.  $E_i$  is the energy of electron in the  $i^{\text{th}}$  states. The real part of the dielectric function  $\epsilon_1(\omega)$  can be extracted from the imaginary part of the dielectric function  $\epsilon_2(\omega)$  by using the Kramers–Kronig relation [26]

$$\epsilon_1(\omega) = 1 + \frac{2}{\pi} P \int_0^\infty \frac{\omega' \epsilon_2(\omega') d\omega'}{(\omega'^2 - \omega^2)}, \quad (3)$$

where  $P$  implies the principal value of the integral. The optical reflectivity spectrum  $R(\omega)$  is calculated for normal incidence on the crystal surface to the optical axis using the relation [26, 27].

$$R(\omega) = \left| \frac{\sqrt{\epsilon(\omega)} - 1}{\sqrt{\epsilon(\omega)} + 1} \right|^2. \quad (4)$$

We have used a Lorentz broadening of 0.1 eV. The calculated optical properties for  $\text{Be}_x\text{Zn}_{1-x}\text{Se}$  alloys for different concentrations have been shifted by a scissor operator shift (SOS) [34]. The currently used SOS is entirely different from the self-energy scissor operator discussed by Fiorentini and Baldereschi [35] and the self-energy shift of Fleszar and Hanke [14]. We simply shift the calculated spectrum rigidly by a certain energy so as to match the onset of  $\epsilon_2(\omega)$  with the measured spectrum. The values of the SOSs for different concentrations are presented in table 3.

The SOSs are used for all five concentrations  $x$  because it is well known that LDA/GGA underestimates the energy band gap. This is due to the fact that the one electron energy spectrum obtained by the LDA/GGA does not express the quasi-particle spectrum. To overcome this problem, the electron self-energy ( $\Sigma$ ) should be estimated precisely. This can be done either by using a many-body perturbation theory approach (MBPT) [36] or time-dependent density functional theory (TDDFT) [37]. The MBPT combines the GW approach [38] for single quasi-particle states with the Bethe–Salpeter equation (BSE) [39] approach for the excitonic contribution. A GW calculation requires quasi-particle energies and amplitudes, taking for  $\Sigma$  the product of the Green function  $G$  and the screened Coulomb interaction  $W$ . An alternative approach for computing neutral excitations is TDDFT, and this is expected to be more efficient than the MBPT-based approach. Sottile [40] has made a comparative study of optical properties using these techniques. These calculations require very heavy computations. Hence, as mentioned earlier, we have used a very simple and empirical SOS [34] in this work to correct the energy gap.

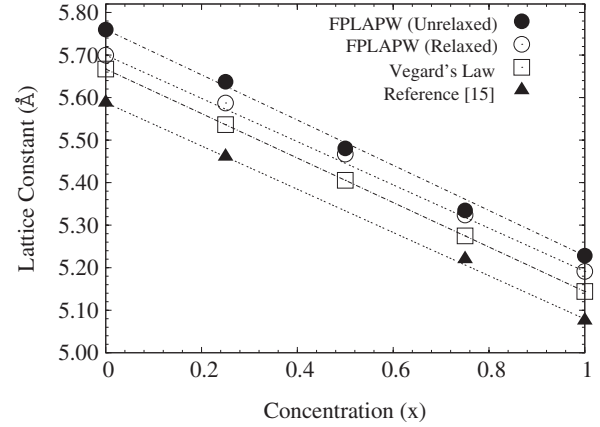


**Figure 1.** Calculated equilibrium lattice constants of  $\text{Be}_x\text{Zn}_{1-x}\text{Se}$  alloys for different concentrations. Filled circles, open circles, open boxes and filled triangles correspond to present calculations with unrelaxed atomic positions, relaxed atomic positions, experimental lattice constants [14, 30] using Vegard’s law and SIESTA results [15], respectively.

### 3. Results and discussion

#### 3.1. Structural parameters

We have used the WIEN2K code [20] to calculate the lattice constants for five values of  $x$  in the  $\text{Be}_x\text{Zn}_{1-x}\text{Se}$  system, although experimental values of the lattice constants are for  $x = 0.0$  and  $x = 1.0$  and linearly interpolated (Vegard’s law) values for  $x = 0.25, 0.50$  and  $0.75$  are used in present calculation. The obtained lattice constants compared with other calculations are presented in table 1. In figure 1, we present our calculated lattice constants as a function of Be concentration along with Vegard’s law and SIESTA [15] results. The calculated lattice constants scale linearly with composition, thus obeying Vegard’s law. The results obtained by FPLAPW (unrelaxed), FPLAPW (relaxed), Vegard’s law and SIESTA [15] are fitted by the linear equations (5), (6), (7), and (8), respectively.

$$a \text{ (Å)} = 5.7598 - 0.5316x \quad (5)$$

$$a \text{ (Å)} = 5.6998 - 0.5085x \quad (6)$$

$$a \text{ (Å)} = 5.667 - 0.5230x \quad (7)$$

$$a \text{ (Å)} = 5.5879 - 0.5123x. \quad (8)$$

Recently, a plane wave pseudopotential calculation [17] also suggested that the lattice constants obey Vegard’s law. We note that there is good agreement between the different methods with a maximum difference of 1.7% for  $x = 0.25$ . Our calculated lattice constants for a relaxed structure show a deviation of 0.56% to 1.38% from Vegard’s law. Our calculations suggest that we are justified in using the lattice constants obtained from Vegard’s law to calculate the optical properties of the  $\text{Be}_x\text{Zn}_{1-x}\text{Se}$  alloys.

**Table 2.** Calculated band gaps for  $\text{Be}_x\text{Zn}_{1-x}\text{Se}$  alloys along  $\Gamma-\Gamma$  and  $\Gamma-X$  symmetry point (all in eV).

System	Present calculation		Previous study	Experimental	
	$(\Gamma-\Gamma)$	$(\Gamma-X)$	$(\Gamma-\Gamma)$	$(\Gamma-\Gamma)$	$(\Gamma-X)$
ZnSe	1.14	2.98	1.04 <sup>a</sup> , 2.41 <sup>b</sup> , 2.69 <sup>b</sup> , 1.11 <sup>c</sup>	2.58 <sup>d</sup>	
$\text{Be}_{0.25}\text{Zn}_{0.75}\text{Se}$	1.90	2.83	1.64 <sup>c</sup>	3.5 <sup>e</sup>	
$\text{Be}_{0.50}\text{Zn}_{0.50}\text{Se}$	2.54	2.72	2.27 <sup>c</sup>	3.95 <sup>e</sup>	
$\text{Be}_{0.75}\text{Zn}_{0.25}\text{Se}$	3.35	2.65	2.75 <sup>c</sup>	4.4 <sup>f</sup>	
BeSe	4.30	2.63	4.37 <sup>g</sup> , 5.47 <sup>h</sup>	5.55 <sup>j</sup> , 4.72 <sup>i</sup> , 4.19 <sup>c</sup>	4.0 <sup>k</sup>

<sup>a</sup> Reference [28]; <sup>b</sup> Reference [41]; <sup>c</sup> Reference [13]; <sup>d</sup> Reference [42];

<sup>e</sup> Reference [8]; <sup>f</sup> Reference [8] for  $\text{Be}_{0.67}\text{Zn}_{0.33}\text{Se}$ ; <sup>g</sup> Reference [12];

<sup>h</sup> Reference [14]; <sup>i</sup> Reference [11]; <sup>j</sup> Reference [9]; <sup>k</sup> Reference [49].

### 3.2. Projected density of states

The projected density of states (PDOS) for different concentrations, i.e.  $x = 0.0, 0.50$  and  $1.0$ , of  $\text{Be}_x\text{Zn}_{1-x}\text{Se}$  alloys are presented in figure 2 with the zero of energy corresponding to the Fermi level or top of the valence band. There is an overall qualitative agreement with earlier first-principles calculations [28, 29]. The PDOS for  $x = 0.0$ , i.e. ZnSe, presented in figure 2(a) can be divided into four regions. In the first region A ( $-13.5$  to  $-4.0$  eV) three sharp structures at  $-12.5$ ,  $-6.4$  and  $-4.7$  eV are visible. A sharp peak structure at  $-12.5$  eV arises due to Se-s states, its nature remains unchanged with increasing Be concentration ( $x$ ) except that the small contribution from Zn-s, -p, -d is replaced by Be-s, and -p states. The second peak at  $-6.4$  eV originates mainly from the strong hybridization of Zn-d and Se-p. The width of the peak ( $-6.4$  eV) decreases with increasing Be concentration. The third structure at  $-4.7$  eV is due to strong hybridization between Se-p and Zn-s, -d states. For  $x = 0.25$  and  $x = 0.50$  the peak broadens, and with further increase in  $x$  it becomes sharp and finally disappears. The second region B ( $-4.0$  to  $0.0$  eV, i.e. the top of the valence band) is mainly due to Se-p states. The third region C (from bottom of the conduction band to  $4.5$  eV) is composed of Zn-s and Se-p states. The fourth region D (from  $4.5$  eV onwards) is dominated by Se-p and Zn-p states.

Our calculations show that replacing Zn by Be causes the bandwidth of the valence band to increase slightly. The character at the top of the valence band remains unchanged. New structures are visible in the C and D regions which are attributed to Be-s, -p states extending from minima of the conduction band to  $6.5$  eV. This clearly indicates that Be-s, -p states should not be treated as localized states. The conduction band minima changes from Zn-s to Be-p states as beryllium is added. The calculated band gap along the  $\Gamma-\Gamma$  symmetry direction increases linearly, while along  $\Gamma-X$  the symmetry direction decreases with Be concentration presented in table 2. The direct to indirect band gap cross-over is equal to  $x \approx 0.53$  in contrast to the measured value [8] of  $x = 0.46$ . In table 2, we compare our results with the results of other calculations and experiments.

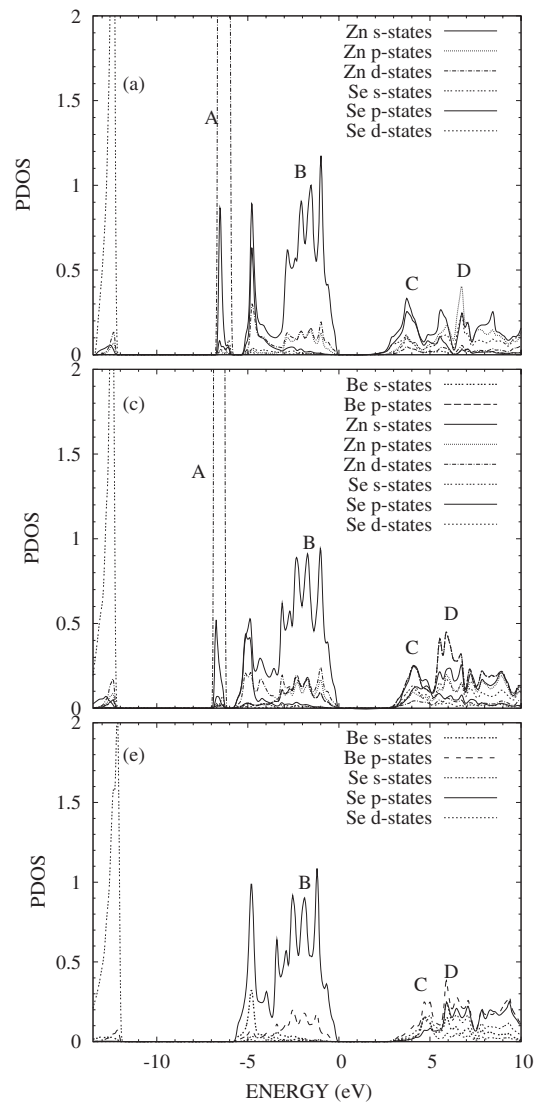


**Figure 2.** Calculated PDOS for  $\text{Be}_x\text{Zn}_{1-x}\text{Se}$  alloys for three different concentrations, i.e.  $x = 0.0, 0.50$  and  $1.00$ .

### 3.3. Imaginary part of the dielectric function

The calculation of  $\epsilon_2(\omega)$  requires energy eigenvalues and electron wavefunctions. These are natural outputs of the band

**Table 3.** Approximate peak positions  $\varepsilon_2(\omega)$  for  $\text{Be}_x\text{Zn}_{1-x}\text{Se}$  alloys (all in eV).

System	Scissor correction	A	B	C
ZnSe	0.600	2.6	4.5	6.0
$\text{Be}_{0.25}\text{Zn}_{0.75}\text{Se}$	0.510	3.0	4.5	6.2
$\text{Be}_{0.50}\text{Zn}_{0.50}\text{Se}$	0.310	4.0	5.0	6.2
$\text{Be}_{0.75}\text{Zn}_{0.25}\text{Se}$	0.150	4.2	5.4	6.2
BeSe	0.175		6.0	6.2

structure calculations. In this section we present calculations for  $\varepsilon_2(\omega)$  and compare them with the available experimental data [9]. We will try to analyze the structures in  $\varepsilon_2(\omega)$  in terms of the projected density of states. In figure 3, the calculated  $\varepsilon_2(\omega)$  are presented for  $\text{Be}_x\text{Zn}_{1-x}\text{Se}$  alloys with and without relaxing the atomic positions for different concentrations, i.e.  $x = 0.0, 0.25, 0.50, 0.75$  and  $1.0$ . These calculated  $\varepsilon_2(\omega)$  are compared with the measured [9] dielectric functions for concentrations of  $x = 0.0, 0.30, 0.50, 0.70$  and  $1.0$ . All the compounds show three structures labeled A, B and C. The location of these structures in the  $\text{Be}_x\text{Zn}_{1-x}\text{Se}$  alloys is given in table 3.

Walter *et al* [43] and Kim *et al* [44] have calculated  $\varepsilon_2(\omega)$  for  $x = 0.0$ , i.e. ZnSe. Our calculations are in agreement with these earlier calculations. The calculated  $\varepsilon_2(\omega)$  for  $x = 0.0$  presented in figure 3(a) has a small peak at 2.6 eV. This could be due to transitions from occupied Se-p states to the unoccupied Zn-s state of the conduction band. The sharp rise in  $\varepsilon_2(\omega)$  at 4.0 eV reaches a maximum at B. This maximum could arise from transitions from just below  $E_F$  Se-p and Se-d states to just above it, i.e. Zn-s and Se-p states. The structure C is dominated by the transitions from Se-p and Zn-s states (4.0 to 6.7 eV) below  $E_F$  to the Se-p and Zn-p states (3.0 eV) above  $E_F$ . We note that with increasing Be concentration  $x$  the conduction band minimum moves towards higher energies (see figure 2). This causes structures A and B to move towards higher energies and finally merge with the structure C for BeSe (see table 3). The shifting of the peaks with increasing  $x$  is consistent with PL data [8]. The structure C arises due to transitions from deep valence states like Se-p and Zn-s,d/Be-s, -p states to conduction band Se-p and Zn-p/Be-s, -p state. The overall main features of  $\varepsilon_2(\omega)$  remain unchanged except that some structures broaden a little.

The measurements have been done for the disordered samples while our calculations are for an ordered crystal. The electronic properties of ordered structures of crystal with impurities sensitively reflect the details of the microscopic atomic arrangements including small changes in atomic positions called relaxation. On the other hand, the obvious difficulty with structural theories of alloys arises from the fact that even in the simplest case of a binary system with  $N$  sites, there are  $2^N$  possible atomic configurations whose total energy needs to be structurally relaxed then averaged. One then needs in practice to either select a representative configuration or a large number of configurations/large cell sizes for which first-principles self-consistent calculations are still impractical. In the present case, we have opted for the first option, i.e. we took three representative configurations for  $x = 0.25, 0.50$  and  $0.75$ .

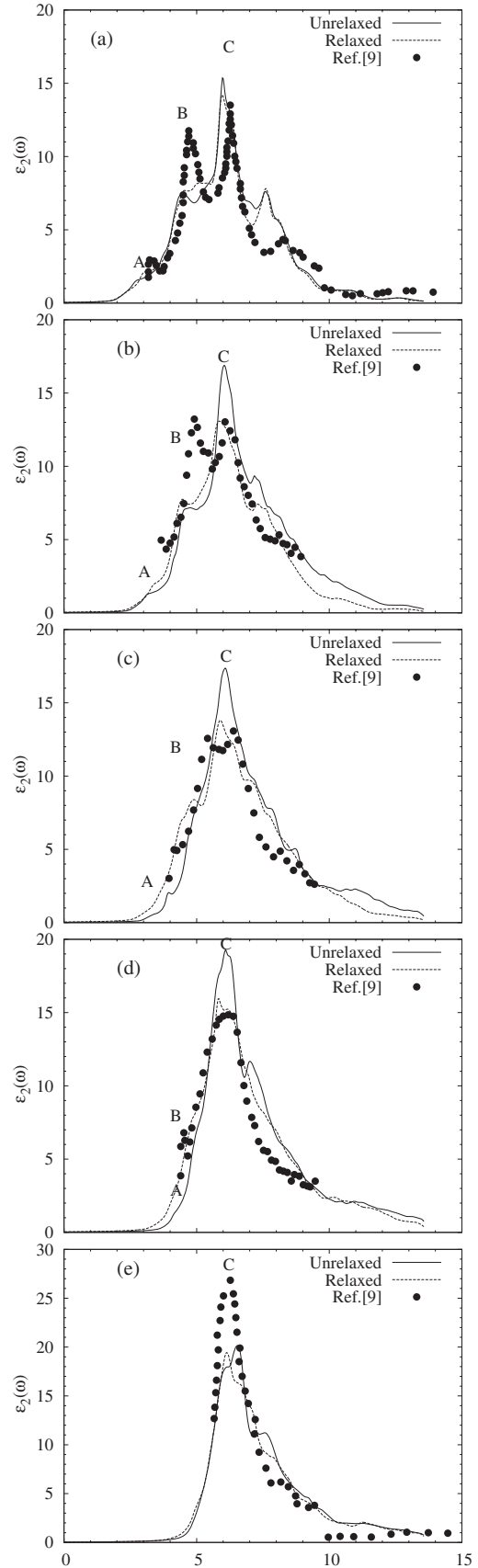


**Figure 3.** Calculated (experimental [9])  $\varepsilon_2(\omega)$ , for  $\text{Be}_x\text{Zn}_{1-x}\text{Se}$  alloys for five different concentrations, i.e.  $x = 0.0$  (0.0),  $0.25$  (0.30),  $0.50$  (0.50),  $0.75$  (0.70) and  $1.0$  (1.0). ( ) are the corresponding experimental values of  $x$ .

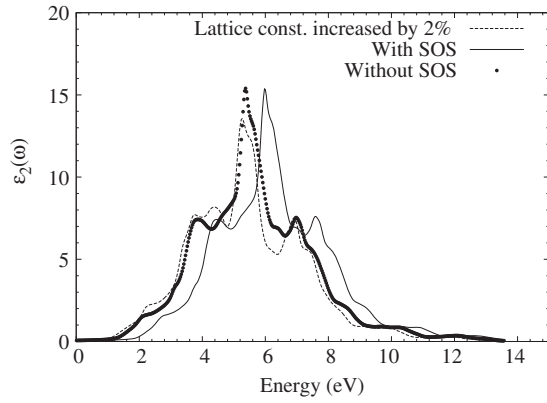


**Figure 4.** Calculated  $\epsilon_2(\omega)$  for ZnSe with SOS (without SOS) and with the lattice constant increased by 2% are presented by the solid line (filled circles) and dashed line, respectively.

The total energies are calculated for all the three systems with and without relaxation of the atomic positions. It is true that there are minor changes in the atomic position of the order of 0.01 au for  $x = 0.50$ , or even less.

The second option, which is beyond the scope of the present calculation, is to choose random alloys. Describing random alloys by a periodic structure will clearly introduce spurious corrections beyond a certain distance. However, many physical properties of solids are characterized by a microscopic length scales that can be ordered by size to form a hierarchy. In general, interactions between distant neighbors contribute less to the total energy than do interaction between close neighbors. Hence, construction of a special quasi-random structure (SQS) [45] by the principle of close reproduction of the perfectly random network for the first few shells around a given site defers periodicity error to more distant neighbors. This approach is similar to guiding the selection of special points for Brillouin zone integration.

It is known that disorderliness leads to an increase in the possibility of indirect optical transitions and violates translational symmetry. We have taken a very simplified view that disorder can be modeled by introducing broadening. We find reasonable agreement with the experimental data for alloys, in contrast to ZnSe. In the measured spectra of ZnSe the second structure at B could be due to excitonic effects [46, 47]. As a matter of fact, excitonic effects are not included in the present calculation. A similar problem with Si optical spectra has been discussed and solved satisfactorily by Sottile [40] taking into account excitonic effects.

$\epsilon_2(\omega)$  for ZnSe is presented in figure 4, with and without SOS, in order to see the effect of SOS on the calculated spectrum. In order to determine the variation of optical properties with lattice constant, we have performed calculations by increasing the lattice constant by 2% (this is around the 1.7% error mentioned above). These are presented in figure 4. There is a minor shift of the spectrum edge while the main structure remains the same. Hence a 1.7% change in the lattice constant is not expected to change the optical properties significantly.

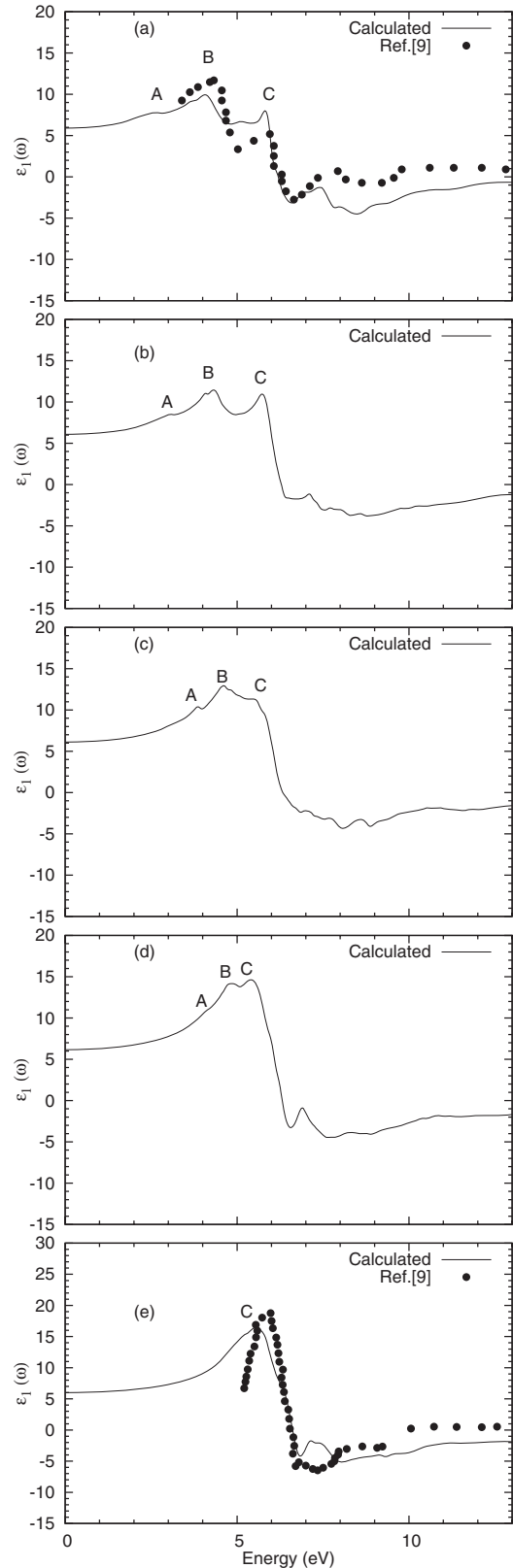


**Figure 5.** Calculated (experimental [9])  $\epsilon_1(\omega)$  for  $\text{Be}_x\text{Zn}_{1-x}\text{Se}$  alloys for five different concentrations, i.e.  $x = 0.0$  (0.0), 0.25, 0.50, 0.75 and 1.0 (1.0). (•) are the corresponding experimental values of  $x$ .

### 3.4. Real part of the dielectric function

The real part of dielectric function  $\epsilon_1(\omega)$  for  $\text{Be}_x\text{Zn}_{1-x}\text{Se}$  alloys for  $x = 0.0, 0.25, 0.50, 0.75$  and 1.0 is presented

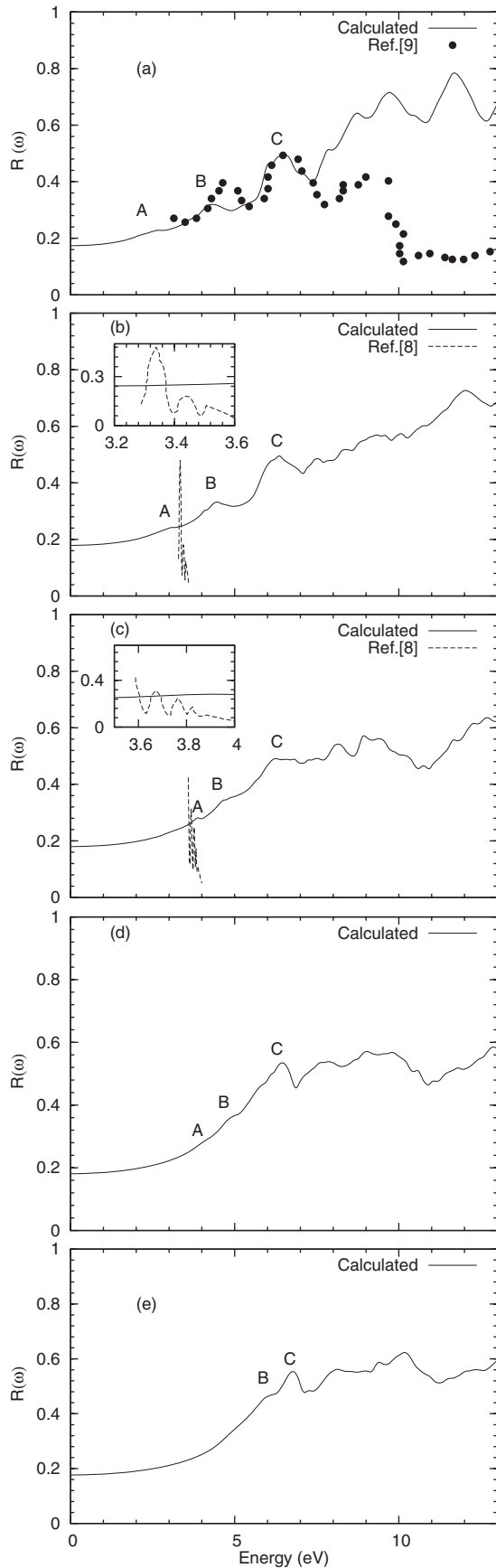


**Figure 6.** Calculated (experimental [8, 9])  $R(\omega)$  for  $\text{Be}_x\text{Zn}_{1-x}\text{Se}$  alloys for five different concentration, i.e.  $x = 0.0$  (0.0), 0.25 (0.31), 0.50 (0.45), 0.75 and 1.0. ( ) are the corresponding experimental values of  $x$ .

in figure 5 along with the available experimental data [9] for  $x = 0.0$  and 1.0. The calculated  $\epsilon_1(\omega)$  for  $x = 0.0$  and 1.0, i.e. ZnSe and BeSe, shows overall good agreement with the measured spectra [9].

### 3.5. Reflectivity

In order to make a more detailed comparison between theory and experiment, we have calculated the frequency dependent reflectivity  $R(\omega)$  for the alloys. The results of our calculations are presented in figure 6. We can identify the three structures A, B and C in figures 5 and 6 as in figure 3 for  $\epsilon_2(\omega)$ . These structures seem to show similar trends as discussed for  $\epsilon_1(\omega)$  and  $\epsilon_2(\omega)$ . For  $x = 0.0$ , the calculated  $R(\omega)$  is compared with the measured experimental data [48]. Chauvet *et al* [8] have measured  $R(\omega)$  in the small energy window 0.3 eV for  $\text{Be}_{0.31}\text{Zn}_{0.69}\text{Se}$  and  $\text{Be}_{0.45}\text{Zn}_{0.55}\text{Se}$ , and values are located above and below structure A in figures 6(b) and (c), respectively. The measured PL structures shift towards higher energies [8] on increasing  $x$  which is consistent with our calculations.

## 4. Conclusions

In this paper, we have presented calculations of the optical properties of the  $\text{Be}_x\text{Zn}_{1-x}\text{Se}$  alloys using the WIEN2K code. We find reasonably good agreement with the available experimental data. We are able to get trends in  $\epsilon_2(\omega)$  that are in agreement with the experimental data. We would like to stress that our calculations are for the ordered alloys while the experimental data are for disordered alloys. Our calculations are performed with GGA and we have not included any electron self-energy corrections. In spite of the simplifications we have used in our approach, the agreement with the experimental data is very encouraging.

## Acknowledgments

Calculations have been performed with the Intel Supermicro Xeon processor based computer. One of us (S Kumar) would like to thank Professor P Blaha for providing a WIEN2K user's license. The Department of Science and Technology and University Grants Commission, New Delhi are acknowledged for their financial support.

## References

- [1] Waag A *et al* 1998 *J. Cryst. Growth* **184/185** 1
- [2] Verie C 1998 *J. Cryst. Growth* **184/185** 1061
- [3] Maruyama K *et al* 2000 *J. Cryst. Growth* **214/215** 104
- [4] Bousquet V *et al* 1997 *Appl. Phys. Lett.* **70** 3564–6
- [5] Guo S P *et al* 2000 *J. Cryst. Growth* **208** 205
- [6] Kim S B *et al* 2001 *Appl. Phys. Lett.* **78** 4151
- [7] Mintairov A M *et al* 1999 private communication
- [8] Chauvet C *et al* 2000 *Phys. Rev. B* **61** 5332
- [9] Wilmers K *et al* 1999 *Phys. Rev. B* **59** 10071



- [10] Stukel D J 1970 *Phys. Rev. B* **2** 1852
- [11] Díaz González M *et al* 1997 *Phys. Rev. B* **55** 14043–6
- [12] Okoye C M I 2004 *Eur. Phys. J. B* **39** 5–17
- [13] Baaziz H *et al* 2006 *Phys. Status Solidi b* **243** 1296–305
- [14] Fleszar A and Hanke W 2000 *Phys. Rev. B* **62** 2466
- [15] Postnikov A V *et al* 2005 *Phys. Rev. B* **71** 115206
- [16] Soler J M *et al* 2002 *J. Phys.: Condens. Matter* **14** 2745
- [17] Berghout A *et al* 2007 *Phys. Rev. B* **75** 205112
- [18] Baroni S *et al* 2005 *Plane Wave Self Consistent Field* <http://www.pwscf.org>
- [19] Singh D J 1994 *Planewaves Pseudopotentials and the LAPW Method* (Boston, MA: Kluwer–Academic)
- [20] Blaha P *et al* 2001 *Computer code WIEN2k* Vienna University of Technology which was published by P Blaha updated Unix/Linux version of the original copyrighted WIEN code Schwartz K *et al* 1990 *Comput. Phys. Commun.* **59** 339
- [21] Perdew J P *et al* 1996 *Phys. Rev. Lett.* **77** 3865
- [22] Agrawal B K *et al* 1997 *J. Phys.: Condens. Matter* **9** 1763–75
- [23] Almeida J S and de Ahuja R 2006 *Appl. Phys. Lett.* **89** 2006
- [24] Jepsen O and Anderson O K 1971 *Solid State Commun.* **9** 1763
- [25] Draxl C A and Abt R 1998 *ICTP Lecture Notes* unpublished
- [26] Wooten F 1972 *Optical Properties of Solids* (New York: Academic)
- [27] Delin A *et al* 1996 *Phys. Rev. B* **54** 1673
- [28] Agrawal Bal K *et al* 1994 *Phys. Rev. B* **50** 14881
- [29] Lee G D *et al* 1995 *Phys. Rev. B* **52** 1459
- [30] Wyckoff R W 1963 *Crystal Structure* 2nd edn (New York: Interscience)
- [31] Okuyama H *et al* 1998 *Phys. Rev. B* **57** 2257
- [32] Hamdi I *et al* 2006 *Phys. Rev. B* **73** 2006
- [33] Waag A *et al* 1996 *J. Appl. Phys.* **80** 792
- [34] Levine Z H and Allan D C 1989 *Phys. Rev. Lett.* **63** 1719
- [35] Fiorentini V and Balderschi A 1995 *Phys. Rev. B* **51** 17196
- [36] Fetter A L and Walecka J D 1971 *Quantum Theory of Many-Particle System* (New York: McGraw-Hill)
- [37] Runge E and Gross E K U 1984 *Phys. Rev. Lett.* **52** 997
- [38] Hedin L 1965 *Phys. Rev. B* **139** A796
- [39] Onida G *et al* 2002 *Rev. Mod. Phys.* **574** 601
- [40] Sottile F 2003 *PhD Thesis* (private communication)
- [41] Luo W *et al* 2002 *Phys. Rev. B* **66** 195215
- [42] Weast R C *et al* 1990 *CRC Handbook of Chemistry and Physics* 70th edn, ed R C Weast *et al* (Boca Raton, FL: CRC Press)
- [43] Walter J P *et al* 1970 *Phys. Rev. B* **1** 2661
- [44] Kim Charles C and Sivananthan S 1996 *Phys. Rev. B* **53** 1475
- [45] Alex Z *et al* 1989 *Phys. Rev. Lett.* **65** 3
- [46] Albrecht S *et al* 1998 *Phys. Rev. Lett.* **80** 4510
- [47] Benedict L X *et al* 1998 *Phys. Rev. Lett.* **80** 4514
- [48] Freeouf J L 1973 *Phys. Rev. B* **7** 3810
- [49] Yim W M *et al* 1972 *J. Phys. Chem. Solids* **33** 501